A histological evaluation on osteogenesis and resorption of methotrexate-loaded calcium phosphate cement *in vivo*

2010 Biomed. Mater. 5 025007

(http://iopscience.iop.org/1748-605X/5/2/025007)

IOP PUBLISHING BIOMEDICAL MATERIALS

Biomed. Mater. **5** (2010) 025007 (7pp) doi:10.1088/1748-6041/5/2/025007

A histological evaluation on osteogenesis and resorption of methotrexate-loaded calcium phosphate cement *in vivo*

Dong Li[1,3,4], Zhiping Yang[1,3,4,5], Xin Li[1], Zhenfeng Li[1], Jianmin Li[1] and Jingyan Yang[2]

[1] Department of Orthopedics, Qilu Hospital of Shandong University, Shandong, People's Republic of China

[2] Department of Pathology, 2nd Affiliated Hospital of Shandong University, Shandong, People's Republic of China

E-mail: yangzhiping@medmail.com.cn

Received 20 October 2009
Accepted for publication 15 February 2010
Published 25 March 2010
Online at stacks.iop.org/BMM/5/025007

Abstract

In this study, we investigated the resorption of *in vivo* methotrexate-loaded calcium phosphate cement (MTX-CPC) implants and their effect on osteogenesis. MTX-CPC implants containing 1% methotrexate (MTX) (weight/weight) were preset and implanted into the femoral condyle of rabbits. Calcium phosphate cement (CPC) without MTX was used as the control. The femurs were harvested at day 1 and at 1, 3 and 6 months after implantation and radiological examination were performed. Decalcified sections were examined by hematoxylin and eosin (HE) staining, alkaline phosphatase (ALPase) immunohistochemistry and tartrate-resistant acid phosphatase (TRAPase) enzyme histochemistry. Then, we performed histomorphometric analysis, including determination of the percentage of newly formed bone and osteoblast and osteoclast counts. The results indicated that MTX-CPC implants were biocompatible, biodegradable and osteoconducive. However, MTX release from the implantation site inhibited osteogenesis in the initial period; this inhibition weakened with time, and no difference was observed between CPC and MTX-CPC at 6 months after implantation. Hence, MTX-CPC is an excellent material for filling defects and can be used for preparing effective drug delivery systems to achieve local control of invasive bone tumors.

(Some figures in this article are in colour only in the electronic version)

1. Introduction

Owing to its porosity, biocompatibility, biodegradation and osteoconducive properties [1–5], calcium phosphate cement (CPC) has been used as a bone substitute material as well as a carrier in drug delivery systems [6–8].

Antibiotic-loaded calcium phosphate bone cement has been widely used for the treatment and prevention of osteomyelitis [9–13]. This application suggests that CPC can also be used as a carrier of antitumor drugs to control the local recurrence of bone tumors and to reduce chemotherapy-related systemic toxicities [14–16].

In vitro and *in vivo* studies on the kinetics of the methotrexate (MTX)-loaded CPC (MTX-CPC) system indicate that CPC may be used as a supporting vehicle in local chemotherapy of bone tumors such as giant cell tumor or osteosarcoma [16].

Our previous study [17] on MTX-CPC has shown that addition of 1% (weight/weight) MTX did not significantly alter the setting times (including initial and final setting time) of CPC. Although the mechanical properties (including the compressive strength and tensile strength) of the MTX-CPC significantly decreased when 1% MTX was added, the MTX-

[3] Joint first author.
[4] Equally contributed to this work.
[5] Author to whom any correspondence should be addressed.

CPC remained compliant with the minimum requirements for clinical application. *In vitro* and *in vivo* experiments on the release kinetics of MTX confirmed that MTX-CPC was a monolithic matrix system, with a burst effect of MTX release in the initial period after implantation and a sudden drop thereafter. MTX release at a level higher than the minimum effective concentration (1×10^{-8} mol L^{-1}) continued for 2–4 months after implantation [16–18].

However, when used as a chemotherapeutic agent, MTX may influence osteogenesis while inhibiting tumor cells. Few studies have investigated the osteogenic properties of MTX-CPC; therefore, we evaluated the resorption of MTX-CPC and its effect on osteogenesis by examining the activities of osteoclasts and osteoblasts.

2. Materials and methods

2.1. Preparation of samples

We purchased CPC from Rebone Biomaterial Co., Ltd (Shanghai, China); it was composed of a powder phase and a liquid phase, with a liquid-to-powder ratio of 0.4 (weight/weight). The powder contained several calcium phosphates, including tetracalcium phosphate (TTCP), dicalcium phosphate dihydrate (DCPD), and hydroxyapatite (HAP) (weight ratio of TTCP:DCPD:HAP = 1.83:0.86:1.79). The liquid phase was 0.05% phosphoric acid. MTX was purchased from Wanma Pharma Co., Ltd (Zhejiang, China).

We added 100 mg of MTX to 10 g of CPC powder. After thorough hand-mixing, 4 ml of 0.05% phosphoric acid was added to this mixture, and the resulting paste was poured into cylindrical molds with diameter 3 mm and height 10 mm. These samples (MTX-CPC) were maintained at 37 °C and 100% relative humidity under light-free conditions for 48 h. Then, the samples were removed and weighed (mean weight, 0.135 g); each sample contained approximately 1.02 mg MTX. CPC samples without MTX were used as control (indicated as CPC).

2.2. Animals and graft

Twenty-four male New Zealand rabbits with an average weight of 3.0 kg were randomly divided into two groups (CPC and MTX-CPC). The study was approved by the Ethical Committee of the Shandong University.

Implantation was performed under aseptic conditions, and general anesthesia was induced using pentobarbiturate (35 mg kg^{-1}). A 1 cm incision was made on the lateral side of the left thighs. The deep fascia was dissected and a cavity (3 mm diameter) was created on the lateral aspect of left femoral condyle by drilling. After washing the bone cavity, the defect was filled with preset MTX-CPC or CPC, and finally the wound was closed. Only CPC was implanted in the control group. No antibiotics were used after operation. At day 1 and at 1, 3 and 6 months after implantation, three rabbits from each group were killed and their left femurs were harvested.

2.3. X-ray analysis

Radiography was performed to observe the density change of the cement, and to assess the material resorption by comparing the postoperative radiographs at day 1 to the postmortal radiographs at month 6. The femurs were harvested and radiographs were obtained in the caudocranial view. The conditions for obtaining radiographic images were as follows: 55 kV, 3.97 mA s^{-1}, and 40 ms.

2.4. Histological procedures

2.4.1. Histological evaluation. The femoral samples were fixed in 10% neutral buffered formalin, decalcified in ethylenediaminetetraacetic acid (EDTA) for 3 weeks, and embedded in paraffin. The embedded tissue blocks were cut into 4 μm sections and the following examinations were performed.

To determine the extent of osteogenesis, the sections were stained with hematoxylin and eosin (HE), and then observed under a light microscope.

To determine the presence of osteoblasts and osteoclasts, histological sections were analyzed by alkaline phosphatase (ALPase) immunohistochemistry and tartrate-resistant acid phosphatase (TRAPase) enzyme histochemistry, according to the procedures described in previous reports [19, 20]. The sections were deparaffinized with xylene and subsequently treated with 0.1% hydrogen peroxidase for 15 min to inhibit the activity of endogenous peroxidase. Rabbit anti-human ALPase monoclonal antibody (Maxim Biotech Inc., Fujian, China) was applied to the sections at a dilution of 1:100, and the sections were incubated overnight at 4 °C; thereafter, the sections were incubated with horse radish peroxidase (HRP)-conjugated goat anti-rabbit IgG (Maxim Biotech Inc., Fujian, China) at 37 °C for 30 min. The immunological reaction was visualized with diaminobenzidine staining. Subsequently, TRAPase was detected by using the TRAPase kit (Institute of hematology, Tianjin, China), which estimated the TRAPase activity in the osteoclasts. The sections were counterstained faintly with hematoxylin.

2.4.2. Histomorphometric analysis. To quantitatively determine the extent of osteogenesis, we statistically analyzed the histological sections implanted with MTX-CPC and CPC after different post-implantation periods (day 1 and 1, 3 and 6 months). We randomly selected three HE-stained histological sections. Each section was observed under a light microscope at 40× magnification. The analytical software Image-J (NIH, USA) was used for image processing, and new bone volume (NBV) was determined and expressed as percentage according to following equation: new bone volume = (new bone area/original drill defect area) × 100.

To quantitatively determine the number of osteoblasts and osteoclasts, we randomly selected three histological sections that were positive for ALPase and TRAPase. Each section was observed under the light microscope at 400× magnification; for each section, five random fields were analyzed. The number of osteoblasts and osteoclasts per field was expressed as osteoblast index (OBI) or osteoclast index (OCI), respectively.

2.5. Statistical analysis

Data collected from new bone formation measurements and osteoblast and osteoclast counts were expressed as mean ± standard deviation (SD) and statistically analyzed using SPSS13.0. Comparative studies of means were performed using the two-sample *t*-test, with $p < 0.05$ indicating a statistically significant difference.

3. Results

All animals recovered satisfactorily and showed no signs of discomfort or lameness. Clinically and histologically, the implanted biomaterials were well tolerated. Bone tissue around the implant showed normal morphology. No lysis of the newly formed bone or the bony defect edges were observed at any of the time periods. There were no signs of rejection, necrosis or infection after implantation.

3.1. X-ray analysis

The CPC (figure 1(*a*)) and MTX-CPC (figure 1(*b*)) implants at day 1 appeared as opaque calcified shadows in the distal part of femur, and this region showed high density. The implants' margin was sharp and the interface between bone and materials was clear.

The density of CPC (figure 1(*c*)) and MTX-CPC (figure 1(*d*)) had reduced significantly at month 6. The density becomes less uniform. Some residual implant material still showed high density. The low density was close to the density of trabecular bone around the materials. It may be due to resorption of the materials and formation of new bone.

The radiological density change of the cement indicated the degradation of CPC and MTX-CPC.

Figure 1. X-ray showed change of the cement density at 1 day and 6 months after implantation. (*a*) CPC implants at day 1. (*b*) MTX-CPC implants at day 1. (*c*) CPC implants (white arrow) at 6 months. (*d*) MTX-CPC implants (white arrow) at 6 months

3.2. Histological evaluation

Day 1 after implantation (figure 2):

CPC implants (figures 2(*a*)–(*c*)): CPC implants in decalcified sections appeared as non-cellular erythroic structure. The surface of the CPC implant was covered with a thin cell layer. Few weak signals of ALPase-positive osteoblasts were obtained at this stage. No TRAPase-positive osteoclasts were identified.

MTX-CPC implants (figures 2(*d*)–(*f*)): the implanted materials were surrounded by the walls of the cortical bones. The interface between the MTX-CPC implants and host bone was clearly visible. No fibrous tissue envelop or inflammatory response was detected. A small gap was observed between the implanted materials and the bone wall.

One month after implantation (figure 3):

CPC implants (figures 3(*a*)–(*c*)): few amorphous organic components, such as bone matrix, formed on the periphery of the CPC implants. Some bony buds began to invade the implant, and reconstructed the irregular shaped bone margin. In some regions, TRAPase-positive osteoclasts were identified on the surface of CPC, while some ALPase-positive osteoblasts were detected on the surface of the newly formed bone.

MTX-CPC implants (figures 3(*d*)–(*f*)): the shape and volume of the MTX-CPC implants at 1 month after implantation appeared unchanged as compared to those of MTX-CPC implants at day 1 after implantation. The implanted material began to show degradation from the periphery. MTX-CPC implants showed decreased bone matrix and fewer osteoclasts as compared to CPC implants at 1 month after implantation.

Three months after implantation (figure 4):

CPC implants (figures 4(*a*)–(*c*)): the bone matrix formation improved in the periphery and more bony buds exhibited inward invasion of the CPC. The CPC established direct contact with the new bone. TRAPase-positive osteoclasts accumulated on CPC, while many osteoblasts assembled on the new bone.

MTX-CPC implants (figures 4(*d*)–(*f*)): few areas showed the union between the original cortical bony wall and the new bone. However, the interface between the implant and bone was still obvious.

Six months after implantation (figure 5):

CPC implants (figures 5(*a*)–(*c*)): the peripheral bone-defect area was filled with newly formed bone, and the central area still contained CPC. Coupling of linear osteoclasts and osteoblasts was observed between the grafted CPC and

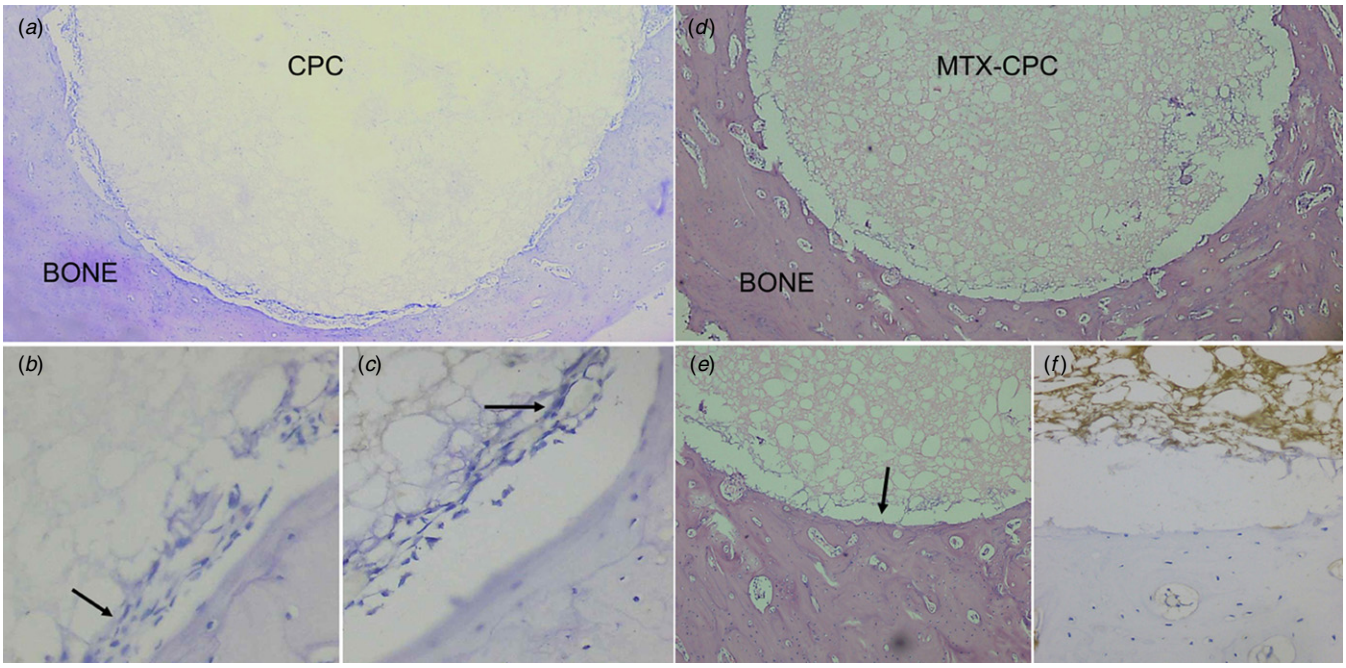

Figure 2. Histological observation of CPC (*a*, *b*, *c*) and MTX–CPC (*d*, *e*, *f*) implants at day 1 after implantation. (*a*) CPC implants in decalcified sections appear like non-cellular erythroic structure. (*b*) The surface of the CPC implants is covered with a thin cell layer (black arrow). (*c*) Few weak signals of ALPase-positive osteoblasts are obtained at this stage (black arrow). No TRAPase-positive osteoclasts are detected. (*d*) The interface between the materials and the host bone is clearly visible. (*e*) A small gap is found between the materials and bony wall (black arrow). (*f*) No ALPase-positive osteoblasts or TRAPase-positive osteoclasts are detected. Magnification: (*a*, *d*) 40×; (*b*, *c*, *e* and *f*) 400×. Staining: (*a*, *b*, *d*, and *e*) HE staining; (*c*, *f*) staining with ALPase and TRAPase.

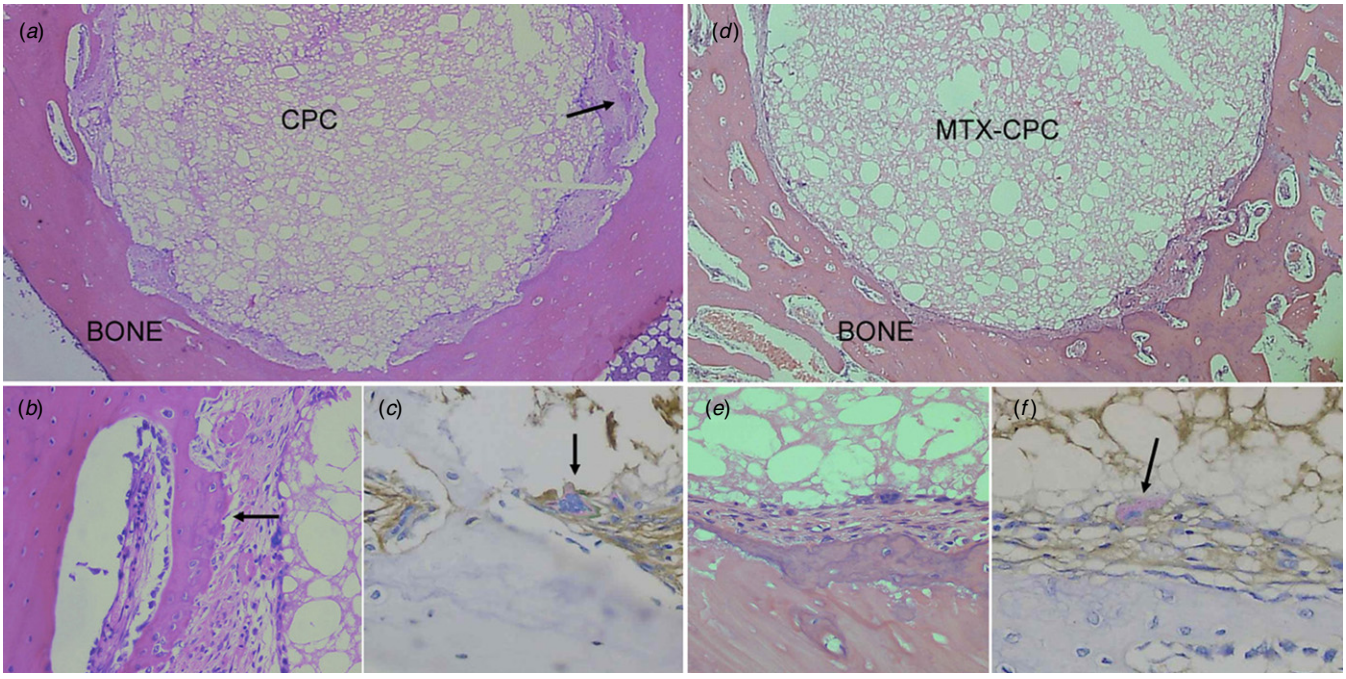

Figure 3. Histological observation of CPC (*a*, *b*, *c*) and MTX-CPC implants (*d*, *e*, *f*) at 1 month after implantation. (*a*) Amorphous organic components, such as bone matrix, formed in periphery (black arrow). (*b*) Invasion of few bony buds into the CPC implants, which reconstructed the irregular shaped margin (black arrow). (*c*) In some regions, TRAPase-positive osteoclasts are identified on the surface of CPC implants (black arrow). (*d*) The shape and volume of the implant materials appears unchanged as compared to those in the CPC-MTXs group at day 1. (*e*) CPC shows degradation from the periphery of the materials. (*f*) The bone matrix and osteoclast count is less than that of CPC implants at 1 month (black arrow). Magnification: (*a*, *d*) 40×; (*b*, *c*, *e*, *f*) 400×. Staining: (*a*, *b*, *d*, *e*) HE staining; (*c*, *f*) staining with ALPase and TRAPase.

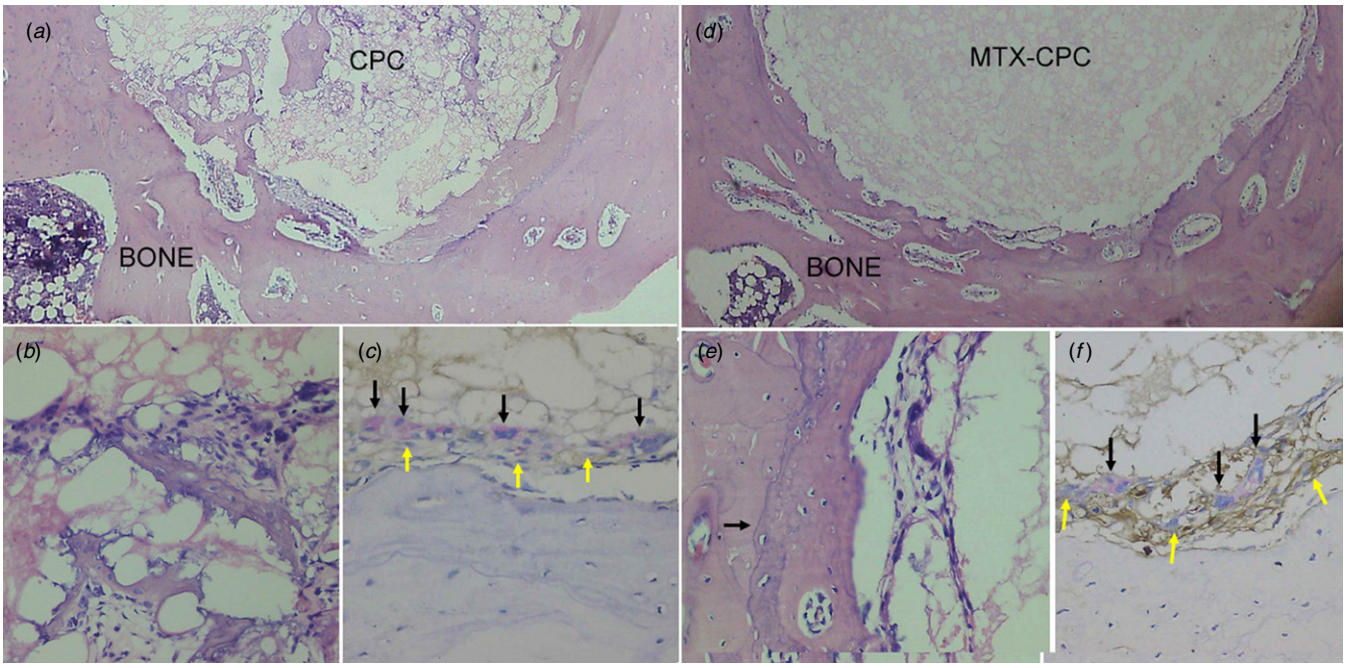

Figure 4. Histological observation of CPC (*a*, *b*, *c*) and MTX–CPC implants (*d*, *e*, *f*) at 3 months after implantation. (*a*, *b*) Improvement of bone matrix formation in the periphery, and more bony buds exhibit inward invasion of the CPC implants. (*c*) Accumulation of TRAPase-positive osteoclasts on CPC implants (black arrow), and assembly of several osteoblasts on the new bone (yellow arrows) is observed. (*d*) The union of the original cortical bony wall and the new bone is observed in some regions. (*e*) However, the interface between the two bones is still distinct (black arrows). (f) Assembly of several osteoclasts (black arrows) and osteoblasts (yellow arrows) on CPC implants. Magnification: (*a*, *d*) 40×; (*b*, *c*, *e*, *f*) 400×. Staining: (*a*, *b*, *d*, *e*) HE staining; (*c*, *f*) staining with ALPase and TRAPase.

Table 1. NBV, OBI, and OCI of CPC and MTX-CPC implants at different times after implantation.

Interval	1 day		1 month		3 months		6 months	
Samples	CPC	CPC-MTX	CPC	CPC-MTX	CPC	CPC-MTX	CPC	CPC–MTX
NBV (%)	0	0	3.98 ± 0.31	2.08 ± 0.46	18.17 ± 3.73	16.51 ± 2.33	38.20 ± 6.87	36.94 ± 2.30
P value				0.004*		0.549		0.778
OBI	0	0	29.13 ± 11.61	20.80 ± 9.14	48.20 ± 14.19	42.07 ± 9.50	69.67 ± 25.82	60.60 ± 22.93
P value				0.038*		0.175		0.318
OCI	0	0	2.73 ± 1.44	1.67 ± 1.14	4.53 ± 2.25	3.00 ± 1.79	5.80 ± 2.54	5.53 ± 2.09
P value				0.034*		0.049*		0.753

*P value for NBV, OBI, or OCI of CPC implants is significantly higher than that of MTX-CPC implants.
NBV: new bone volume (percentage of newly formed bone); OBI: osteoblast index (osteoblast count per field); OCI: osteoclast index (osteoclast count per field).

the new bone. The newly formed bone showed trabecular characteristics. The boundary between the CPC and the host bone was unclear due to the formation of mature bone tissue.

MTX-CPC implants (figures 5(*d*)–(*f*)): the changes in MTX-CPC implants were similar to those observed in CPC implants at 6 months after transplantation. The newly formed bone was still distinguishable from the original bone, and the boundary between these two bones was still distinct.

3.3. Histomorphometric analysis

We performed a quantitative analysis of the newly formed bone. Different histomorphometric parameters determined at various implantation times are presented in table 1. NBV indicates new-bone volume (percentage of newly formed bone); OBI indicates the osteoblast index (osteoblast count per field); OCI indicates the osteoclast index (osteoclast count per field).

At 1 month after implantation, the NBV of CPC implants (3.98%) was significantly higher than that of MTX-CPC implants (2.08%). The OBI and OCI of CPC implants were also significantly higher than those of MTX-CPC implants.

At 3 months after implantation, NBV of both CPC (18.17%) and MTX-CPC implants (16.51%) increased dramatically, and no significant difference was observed between these two values. There was no significant difference between the OBI of CPC and MTX-CPC implants. However, the OCI of CPC implants was still higher than that of CPC-MTX implants.

At 6 months after implantation, the NBV values of CPC and MTX-CPC implants were 38.20% and 36.94%,

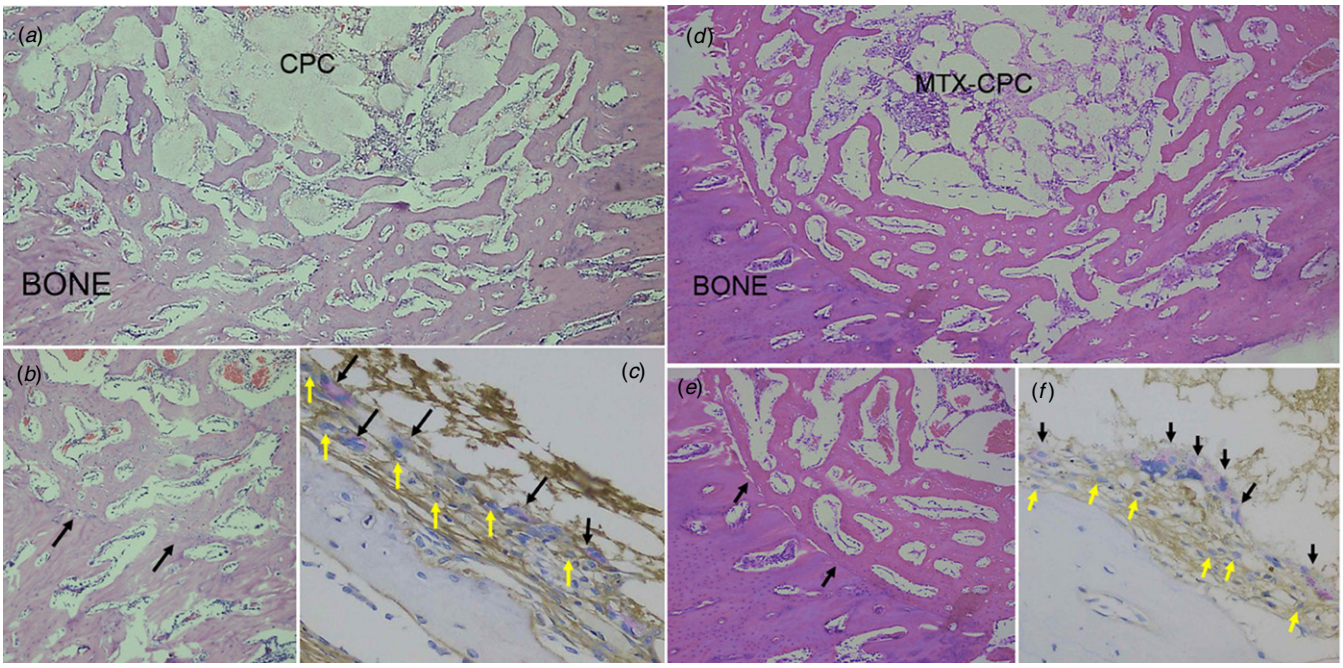

Figure 5. Histological observation of CPC (*a*, *b*, *c*) and MTX-CPC implants (*d*, *e*, *f*) at 6 months after implantation. (*a*, *d*) Peripheral bone-defect area is filled with the newly formed bone and the central area is still occupied by CPC implants. (*b*, *e*) The newly formed bone is still distinguishable from the original bone (black arrows). Unlike the cortical bone at 3 months after implantation, the newly formed bone at 6 months after implantation shows the presence of trabeculae. (*c*, *f*) The coupling of abundant linear osteoclasts (black arrows) and osteoblasts (yellow arrows) is observed between the CPC implants and the new bone. Magnification: (*a*, *d*) 40×; (*b*, *c*, *e*, *f*) 400×. Staining: (*a*, *b*, *d*, *e*) HE staining; (*c*, *f*) staining with ALPase and TRAPase.

respectively. There was no significant difference in the NBV, OBI and OCI values of CPC and MTX-CPC implants.

4. Discussion

The use of bone cement loaded with a chemotherapeutic agent has been proposed as an effective method to fill bone defects and reduce local recurrence of surgically removed invasive bone tumors such as giant cell tumors. However, the osteogenic influence of MTX-CPC systems has not been elucidated. In our study, we implanted preset samples away from the physis to eliminate the influence of the growth plate on osteogenesis.

Our study indicates the biocompatibility of MTX-CPC. Materials were well tolerated and did not cause any foreign body reactions. No inflammatory response or fibrous encapsulation reported in other articles [21–24] was observed on the cement surface in this experiment.

In the present study, x-ray and histological sections demonstrated that both CPC and MTX–CPC showed biodegradability and osteogenesis. New bone formation occurred synchronously with the resorption of the implant material in a creeping substitution process. With the decrease in material volume, new bone growth developed from the periphery to the center. Osteoclast-type cells were responsible for cement degradation [25]. Their phagocytic capacity for calcium-phosphate particles has already been described *in vivo* and *in vitro* [23, 26–28]. In this study, osteoclasts could be found firstly at 1 month on the surface of both materials. At the early stage, osteoclasts accumulated CPC, thereby providing space for the subsequent migration of osteoblasts. Newly formed bone matrix was found at the margins of the resorption zone and continued to expand from the edges into the resorption zone. At the later stage (3 and 6 months after implantation), bone apposition was succeeded by coupling of osteoblasts and osteoclasts with increasing time. Resorption and osteogenesis progress paralleled the increased amounts of osteoclasts and osteoblasts. Union between the original cortical bony wall and the new bone was observed and newly formed bone was found in direct contact with residual materials. These results demonstrated that cell-involved material resorption and new bone formation played an important role in bone repair, with which it seems most authors agreed [24, 26, 27].

However, the NBV of the CPC implant was different from that of the MTX-CPC implant. At 1 month after implantation, the percentage of NBV and the osteoblast and osteoclast counts in the control CPC were significantly higher than those in the MTX-CPC. Further, even at 3 months after implantation, the osteoclast counts of CPC and MTX-CPC were significantly different. These results could be correlated with the release of MTX *in vivo*. Our previous study on *in vitro* and *in vivo* MTX release [17] revealed that the MTX-CPC system was a monolithic matrix system characterized by diffusion and a burst effect, usually in the initial stage. The local concentrations of MTX were 4.57 μg ml^{-1} (10.06 μmol l^{-1}) and 1.13 μg ml^{-1} (2.49 μmol l^{-1}) at 1 and 15 days after implantation, respectively, and thereafter,

MTX was released at a slow rate until the end of the experiment at 30 days (MTX concentration at 30 days after implantation, ~0.37 μg ml^{-1} (0.82 μmol l^{-1})). Based on the MTX concentration on day 30, we estimate that the release could continue for 2–4 months. These results revealed that the release of MTX at concentrations between 0.82 and 10.06 μmol l^{-1} exerted an inhibitory effect on osteogenesis, thus explaining the differences in the new bone area and osteoblast and osteoclast counts for CPC and MTX-CPC implants in the first 3 months after implantation. Further research is warranted to confirm this point.

5. Conclusion

Both CPC and MTX–CPC implants possessed biodegradable and osteoconducive properties. However, the release of MTX could inhibit osteogenesis in the initial period after implantation. We determined that the inhibition progressively weakened and no difference was observed between CPC and MTX-CPC implants at 6 months after implantation. The MTX-CPC implants were absorbed well, and replaced by the newly formed bone. Therefore, MTX-CPC could serve as an excellent material for filling defects and for preparing effective drug delivery systems to achieve the local control of invasive bone tumors.

Acknowledgments

This work is supported by research funds from the Department of Science and Technology of Shandong Province, China.

References

[1] Ooms E M *et al* 2003 Soft-tissue response to injectable calcium phosphate cements *Biomaterials* **24** 749–57
[2] LeGeros R Z 2002 Properties of osteoconductive biomaterials: calcium phosphates *Clin. Orthop. Relat. Res.* **395** 81–98
[3] del Real R P *et al* 2003 *In vivo* bone response to porous calcium phosphate cement *J. Biomed. Mater. Res.* **65** 30–6
[4] Ogose A *et al* 2002 Histological examination of beta-tricalcium phosphate graft in human femur *J. Biomed. Mater. Res.* **63** 601–4
[5] Kondo N *et al* 2005 Bone formation and resorption of highly purified beta-tricalcium phosphate in the rat femoral condyle *Biomaterials* **26** 5600–8
[6] Ginebra M P, Traykova T and Planell J A 2006 Calcium phosphate cements: competitive drug carriers for the musculoskeletal system? *Biomaterials* **27** 2171–7
[7] Sasaki T *et al* 2005 *In vitro* elution of vancomycin from calcium phosphate cement *J. Arthroplasty* **20** 1055–9
[8] Li D X *et al* 2007 Controllable release of salmon-calcitonin in injectable calcium phosphate cement modified by chitosan oligosaccharide and collagen polypeptide *J. Mater. Sci. Mater. Med.* **18** 2225–31
[9] Yu D *et al* 1992 Self-setting hydroxyapatite cement: a novel skeletal drug delivery system for antibiotics *J. Pharm. Sci.* **81** 529–31
[10] Shinto Y *et al* 1992 Calcium hydroxyapatite ceramic used as a delivery system for antibiotics *J. Bone Joint Surg. Br.* **74** 600–4
[11] Bohner M *et al* 1997 Gentamicin-loaded hydraulic calcium phosphate bone cement as antibiotic delivery system *J. Pharm. Sci.* **86** 565–72
[12] Kisanuki O *et al* 2007 Experimental study of calcium phosphate cement impregnated with dideoxy-kanamycin B *J. Orthop. Sci.* **12** 281–8
[13] Otsuka M *et al* 1994 A novel skeletal drug delivery system using self-setting calcium phosphate cement: 2. Physicochemical properties and drug release rate of the cement containing indomethacin *J. Pharm. Sci.* **83** 611–5
[14] Otsuka M *et al* 1994 A novel skeletal drug delivery system using self-setting calcium phosphate cement: 5. Drug-release behavior from a heterogeneous drug-loaded cement containing an anticancer drug *J. Pharm. Sci.* **83** 1565–8
[15] Tahara Y and Ishii Y 2001 Apatite cement containing *cis*-diaminedichloroplatinum implanted in rabbit femur for sustained release of the anticancer drug and bone formation *J. Orthop. Sci.* **6** 556–65
[16] Lebugle A *et al* 2002 Study of implantable calcium phosphate systems for the slow release of methotrexate *Biomaterials* **23** 3517–22
[17] Yang Z P *et al* 2009 Incorporation of methotrexate in calcium phosphate cement: behavior and release *in vitro* and *in vivo* *Orthopedics* **32** 27
[18] Chabner B A and Young R C 1973 Threshold methotrexate concentration for *in vivo* inhibition of DNA synthesis in normal and tumorous target tissues *J. Clin. Invest.* **52** 1804–11
[19] Amizuka N *et al* 1998 Morphological examination of bone synthesis via direct administration of basic fibroblast growth factor into rat bone marrow *Microsc. Res. Tech.* **41** 313–22
[20] Hao H *et al* 2004 A histological evaluation on self-setting alpha-tricalcium phosphate applied in the rat bone cavity *Biomaterials* **25** 431–42
[21] Flautre B *et al* 1999 Volume effect on biological properties of a calcium phosphate hydraulic cement: experimental study in sheep *Bone* **25** 35–9
[22] Kurashina K *et al* 1997 *In vivo* study of calcium phosphate cements: implantation of an α-tricalcium phosphate/dicalcium phosphate dibasic/tetracalcium phosphate monoxide cement paste *Biomaterials* **18** 539–43
[23] Constantz B R *et al* 1998 Histological, chemical, and crystallographic analysis of four calcium phosphate cements in different rabbit osseous sites *J. Biomed. Mater. Res.* **43** 451–61
[24] Lu J X *et al* 1998 Comparative study of tissue reactions to calcium phosphate ceramics among cancellous, cortical, and medullar bone sites in rabbits *J. Biomed. Mater. Res.* **42** 357–67
[25] Chazono M *et al* 2004 Bone formation and bioresorption after implantation of injectable beta-tricalcium phosphate granules–hyaluronate complex in rabbit bone defects *J. Biomed. Mater. Res. A* **70A** 542–9
[26] Malard O *et al* 1999 Influence of biphasic calcium phosphate granulometry on bone ingrowth, ceramic resorption, and inflammatory reactions: preliminary *in vitro* and *in vivo* study *J. Biomed. Mater. Res.* **46** 103–11
[27] Lu J *et al* 2002 The biodegradation mechanism of calcium phosphate biomaterials in bone *J. Biomed. Mater. Res.* **63** 408–12
[28] Pioletti D P *et al* 2000 The effects of calcium phosphate cement particles on osteoblast functions *Biomaterials* **21** 1103–14